



Dynamical robustness in complex networks: the crucial role of low-degree nodes

Gouhei Tanaka^{1,2}, Kai Morino² & Kazuyuki Aihara^{1,2}

¹Institute of Industrial Science, The University of Tokyo, Tokyo 153-8505, Japan, ²Graduate School of Information Science and Technology, The University of Tokyo, Tokyo 113-8656, Japan.

SUBJECT AREAS:

STATISTICAL PHYSICS,
THERMODYNAMICS AND
NONLINEAR DYNAMICS

THEORETICAL PHYSICS

MATHEMATICS

SYSTEMS BIOLOGY

Received
20 September 2011

Accepted
3 January 2012

Published
25 January 2012

Correspondence and
requests for materials
should be addressed to
G.T. (gouhei@sat.t.
u-tokyo.ac.jp)

Many social, biological, and technological networks consist of a small number of highly connected components (hubs) and a very large number of loosely connected components (low-degree nodes). It has been commonly recognized that such heterogeneously connected networks are extremely vulnerable to the failure of hubs in terms of structural robustness of complex networks. However, little is known about dynamical robustness, which refers to the ability of a network to maintain its dynamical activity against local perturbations. Here we demonstrate that, in contrast to the structural fragility, the nonlinear dynamics of heterogeneously connected networks can be highly vulnerable to the failure of low-degree nodes. The crucial role of low-degree nodes results from dynamical processes where normal (active) units compensate for the failure of neighboring (inactive) units at the expense of a reduction in their own activity. Our finding highlights the significant difference between structural and dynamical robustness in complex networks.

Network science has witnessed many developments in the last decade because many real-world networks were found to have a variety of topological structures^{1–3}. The complexity of a network structure can be characterized by the connectivity properties of the interaction pathways (links) between network components (nodes). The degree of a node is the number of its links connected to other nodes. In terms of the degree distribution (the probability distribution of the degrees of all the nodes in the network), complex networks can be classified into homogeneous and heterogeneous networks. Homogeneous networks such as random graphs⁴ and small-world models⁵ possess binomial or Poisson degree distribution, where the degrees concentrate around the mean degree. Heterogeneous networks such as scale-free networks⁶ have a heavy-tailed degree distribution that at least approximately follows a power law. Data analyses have revealed that the scale-free property is found in social^{7,8}, biological^{9–11}, technological^{12,13}, and many other types of networks^{1–3,6}.

One of the major characteristics of heterogeneous networks is that they are highly robust against random errors but are extremely fragile to attacks targeted at hubs¹⁴. Namely, the connectivity properties of a heterogeneous network as a whole are not so much affected by the random removal of a fraction of the nodes as compared with a homogeneous network; however, they are drastically altered by the preferential removal of hubs, leading to network fragmentation. These properties have been theoretically studied by means of percolation theory^{15–17}. The structural fragility to the preferential removal of important nodes is also observed in heterogeneous network models incorporating dynamical flows of physical quantities on the network^{18,19}. Most of these studies are concerned with the robustness of the network structure: the measure of network function is given by the size of the giant component (the largest connected subnetwork), and failure nodes are removed to induce a topological change. However, less attention has been paid to changes in network dynamics caused by local errors in complex networks of dynamical units²⁰, which are particularly relevant to biological robustness^{21,22}. Because most real-world complex networks are composed of elements with internal dynamics, it is essential to consider the robustness with respect to nonlinear dynamics.

Here we focus on the dynamical robustness of complex networks, which is defined as the ability of a network to maintain its dynamical activity when a fraction of the dynamical components are deteriorated or functionally depressed but not removed. Our aim is to demonstrate that the key nodes impacting the dynamical robustness of heterogeneous networks are low-degree nodes. This is in strong contrast to the structural robustness which is largely influenced by hubs. As an example of networks consisting of dynamical units, we introduce coupled oscillator networks^{23–25} which have often been used to study a variety of biological phenomena including circadian rhythms, synchronized neuronal firing, and spatiotemporal activity in the heart and the brain. In the mammalian



suprachiasmatic nucleus (SCN) producing a biological clock that drives circadian rhythms, normal function is sustained by networks of SCN neuronal oscillators²⁶. The self-sustained oscillation of each individual SCN neuron can be damped because of some environmental conditions²⁷ or age-related deterioration²⁸. Coupled oscillator models are useful for exploring how circadian rhythms are robustly generated in a population of self-sustained and damped circadian oscillators²⁹. In the pancreatic islets, synchronized oscillatory activity of electrically coupled beta cells is involved in pulsatile insulin secretion that regulates blood glucose levels. A major issue that has been studied using coupled oscillator models is how rhythmic insulin secretion can be robustly achieved in populations of heterogeneous cells that are active or silent³⁰. There are many other dynamical cellular and multicellular processes in which oscillation plays important roles^{31,32}. Moreover, coupled oscillator models are also relevant to electric power networks in which network components like power sources should be synchronized at the same frequency³³. It is essential to investigate how the collective dynamics of power networks is tolerant to local disturbances of power sources that may lead to a cascading blackout^{34,35}.

We consider networks consisting of N oscillator nodes coupled by diffusive connections with fixed strength K (see Methods section). A normal (active) oscillator exhibits periodic oscillation when it is isolated, whereas a deteriorated (inactive) oscillator settles down in a quiescent state after transient damping oscillation (Fig. 1a)^{36,37}. Unless any local deterioration occurs, the network of all active oscillators produces completely synchronized oscillation. When a proportion of the oscillators are randomly inactivated with ratio p in a heterogeneous network (Fig. 1b), we observe phase synchronized oscillation with different amplitudes (Fig. 1c). The individual inactive oscillator, which cannot oscillate by itself, manages to continue weak oscillation in the network because of continuous inputs from neighboring active oscillators through diffusive coupling. Instead, the active oscillators decrease their oscillation levels as compared with the isolated ones in order to achieve a balance between their states and those of neighboring inactive oscillators.

Results

Behavior in the oscillator network model. The oscillation amplitude of a node is largely dependent on the degree of the node in heterogeneous networks (Fig. 2a), as compared with homogeneous networks (Fig. 2c). When a part of the oscillators are randomly inactivated independently of their degrees, the expected number of inactive oscillators connected to a node is proportional to the degree of the node. Therefore, within the subpopulation of active oscillators, the nodes with lower degree are likely to generate larger oscillation amplitudes because they are less affected by the neighboring inactive oscillators. To measure the network activity, we introduce the order parameter $|Z|$ that represents the average of the oscillation amplitudes over all the oscillators in the phase synchronization state (see Methods section). As the ratio p increases, the order parameter decreases (Figs. 2b and 2d). When p exceeds a critical value p_c , the order parameter vanishes with a loss of global oscillation. For a sufficiently large coupling strength K , the order parameter displays a second-order phase transition at $p = p_c$ ^{36,37}. The critical ratio p_c , namely the maximum inactivation ratio for which the network activity is sustainable, is regarded as a measure of the dynamical robustness. A higher critical value implies a more dynamically robust network.

Random inactivation. In the case where oscillators are randomly inactivated, the critical ratio p_c is analytically obtained for both heterogeneous and homogeneous networks (see Methods section and Supplementary Information). The degree of the j th oscillator is denoted by k_j ($j = 1, \dots, N$) and the mean degree, by $\langle k \rangle \equiv \sum_j k_j / N$. We assume that the behavior of a heterogeneous

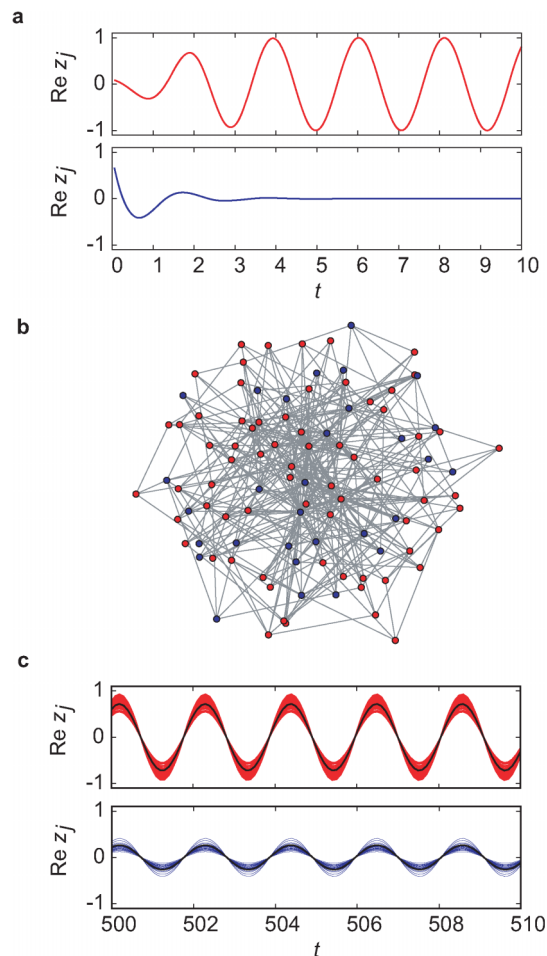


Figure 1 | An oscillator network model. (a) The behavior of the isolated active (red curve) and inactive (blue curve) oscillators. The active oscillator exhibits periodic oscillation, whereas the inactive oscillator becomes quiescent after transient damping oscillation. (b) A heterogeneous network composed of active (red nodes) and inactive (blue nodes) oscillators. Here, the oscillators are randomly inactivated with ratio $p = 0.3$. The link density is $d \sim 0.08$ ($N = 100$ and $\langle k \rangle = 8$). (c) The behavior of $(1 - p)N$ active (red curves) and pN inactive oscillators (blue curves) in the network. The coupling strength is set at $K = 30$. The solid black curve in each panel indicates the mean field for each subpopulation. The inactive oscillators, which are not able to oscillate when isolated, manage to sustain the oscillatory behavior because of the diffusive interactions with neighboring active oscillators. All the oscillators show phase synchronization.

network with large N is governed by two mean fields corresponding to the subpopulations of active and inactive oscillators. In order to apply the degree-weighted mean field approximation^{38,39} or the annealed network approximation⁴⁰ to each subnetwork, we assume that the oscillators with the same degree in the same subpopulation are identical. Under this assumption, the critical ratio p_c for heterogeneous networks is derived as follows:

$$p_c^{\text{het}} = \frac{F(K, a) - d}{F(K, a) - F(K, -b)} \quad \text{for } K > K_c^{\text{het}}, \quad (1)$$

where $d \equiv \langle k \rangle / (N - 1)$ ($\sim \langle k \rangle / N$ for large N) is the link density, K is the coupling strength, and $a > 0$ and $-b < 0$ are the values of the intrinsic parameters for the active and inactive oscillators, respectively (see Methods section). The function F is dependent on the degree distribution normalized by the system size as well as the coupling strength and the intrinsic parameters (see equation (6)). The critical coupling strength, below which $p_c^{\text{het}} = 1$, is given by

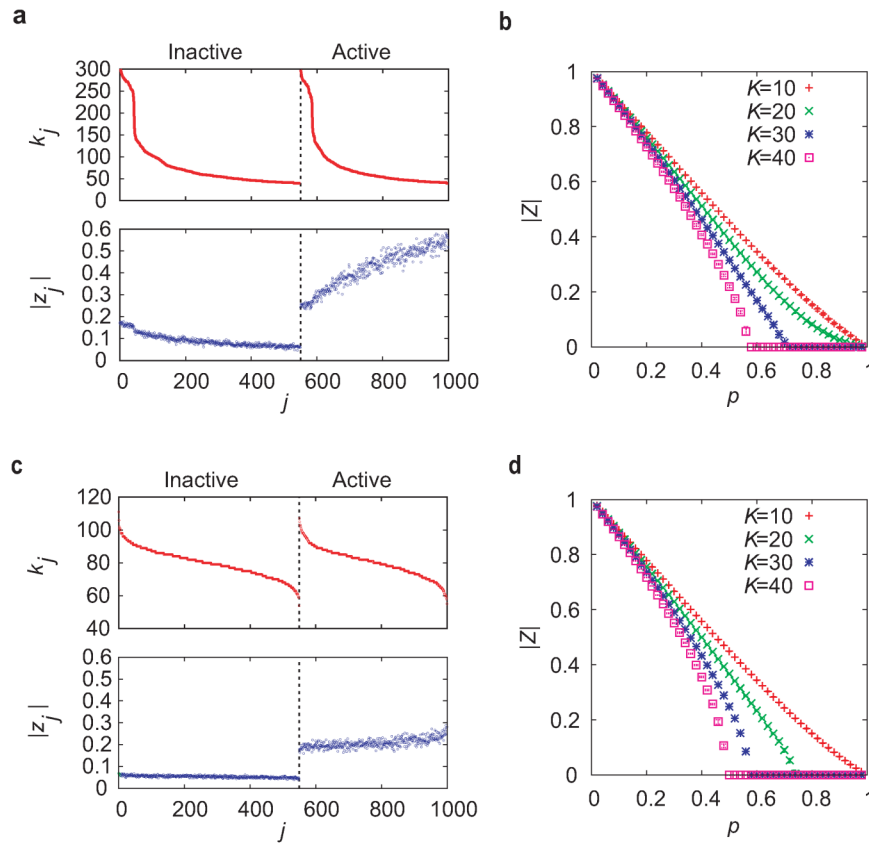


Figure 2 | Behavior in heterogeneous and homogeneous networks. (a), (c) The upper panel shows the degrees k_j of individual oscillators in (a) heterogeneous and (c) homogeneous networks with $d \sim 0.08$ ($N = 1,000$ and $\langle k \rangle = 80$), $K = 30$, and $p = 0.55$. The lower panel shows the oscillation amplitudes $|z_j|$ of the individual oscillators. (b), (d) The order parameter $|Z|$ is plotted against the inactivation ratio p for (b) heterogeneous and (d) homogeneous networks with $d \sim 0.08$ ($N = 1,000$ and $\langle k \rangle = 80$). The critical ratio p_c , at which $|Z|$ reaches 0, is different between the two types of networks for sufficiently large K . The error bars indicating the variance for 10 network realizations are invisibly small.

$K_c^{het} \sim a/d_{min}$, where $d_{min} \equiv k_{min}/N$ with the minimum degree $k_{min} \equiv \min_{1 \leq j \leq N} k_j$. For homogeneous networks, we further assume that the degrees of all the oscillators are approximated by the mean degree for analytical calculations. Then, the critical ratio is described as follows:

$$p_c^{hom} = \frac{a(Kd+b)}{(a+b)Kd} \quad \text{for } K > K_c^{hom}, \quad (2)$$

where $K_c^{hom} = a/d \leq K_c^{het}$. The critical ratio is invariant if the product of the link density and the coupling strength is kept constant. Hence,

a more strongly or densely connected network is less robust. The critical ratios for homogeneous and heterogeneous networks are plotted against the coupling strength K and the link density d in Figs. 3a and 3b. The results of the analytical formulae are in good agreement with the corresponding numerical results. For a wide range of parameter values, the critical ratio for the heterogeneous network is larger than that for the homogeneous network. This property can be further confirmed by the comparison between Fig. 4a for heterogeneous networks and Fig. 4b for homogeneous

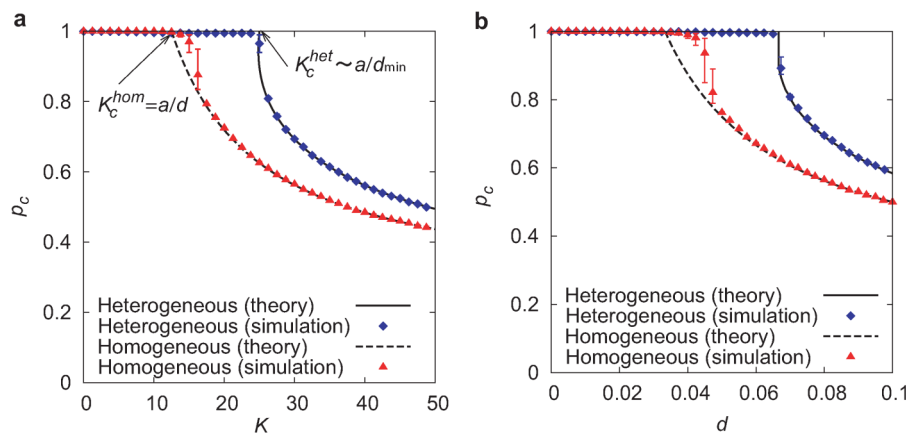


Figure 3 | Comparison of the critical ratio with respect to coupling strength K and link density d between heterogeneous and homogeneous networks for random inactivation. (a) The critical ratio p_c is plotted against the coupling strength K in networks with $d \sim 0.08$ ($N = 3000$ and $\langle k \rangle = 240$). A globally oscillatory state with $|Z| > 0$ is observed for $p < p_c$ whereas a quiescent state with $|Z| = 0$ is observed for $p > p_c$. The solid and dashed black curves indicate the analytically obtained results in equations (1) and (2), respectively. Blue diamonds and red triangles indicate the numerically obtained results. The error bars indicate the variance for 10 network realizations. (b) The critical ratio p_c is plotted against the link density d in networks with $N = 3000$ and $K = 30$.

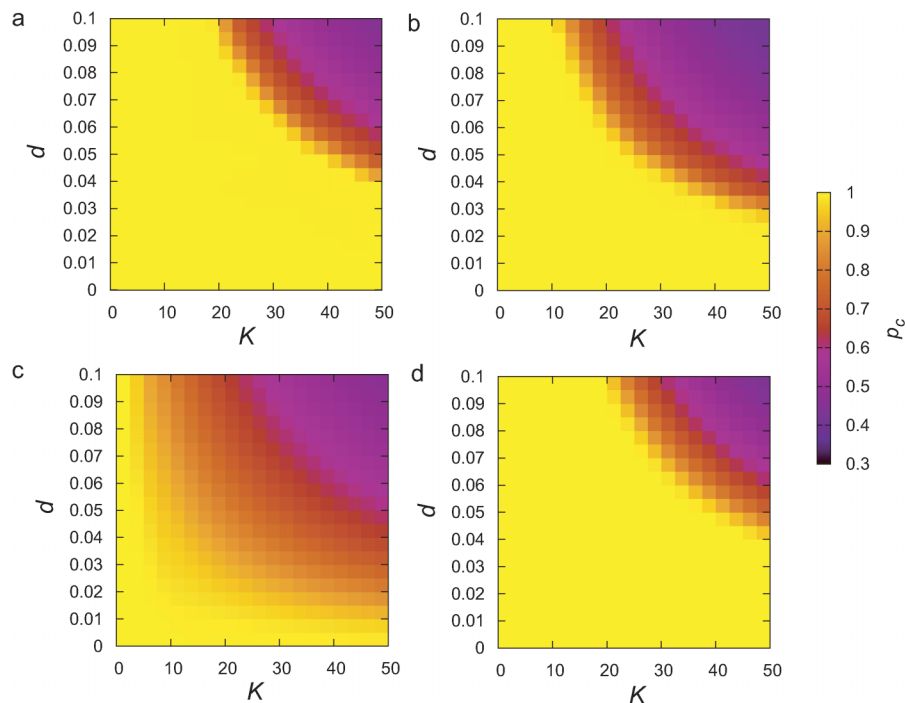


Figure 4 | Dependence of the critical ratio on coupling strength K and link density d . The color indicates the value of the critical ratio p_c in networks with $N = 3000$. (a) Heterogeneous networks for random inactivation. (b) Homogeneous networks for random inactivation. (c) Heterogeneous networks for targeted inactivation of low-degree nodes. (d) Heterogeneous networks for targeted inactivation of high-degree nodes.

networks in the parameter space of K and d . Therefore, heterogeneous networks are more tolerant to random inactivation than homogeneous ones. This result is consistent with that based on the structural robustness against random removal of nodes^{1–3,14–17}.

Targeted inactivation. In the case where oscillators are not randomly inactivated, the mean field approximation is not appropriate. Thus, we numerically computed the critical ratios for preferential inactivation targeted at either high-degree or low-degree nodes in heterogeneous networks. First, the node with the highest (lowest) degree among the active oscillators was inactivated. Then, this process was repeated until the number of inactive oscillators became pN . The critical ratio for targeted inactivation is compared with that for random inactivation in heterogeneous networks, as shown in Figs. 5a and 5b. Compared with the random inactivation case, the targeted inactivation of low-degree nodes makes the networks significantly vulnerable for a wide range of parameter values. This consequence is opposite to the structural fragility against removal of hubs. Figures 4a and 4c also clearly show the difference between the critical ratio p_c for random inactivation and that for targeted inactivation of low-degree nodes. As explained before, the active oscillators with lower degrees are likely to exhibit larger oscillation amplitudes (see Fig. 2a). Therefore, the inactivation of low-degree nodes more dramatically decreases the order parameter and thereby results in a lower critical ratio compared with the random inactivation. The critical coupling strength indicated in Fig. 5a is obtained as $K_c^{het,l} = a/d_{max}$, where $d_{max} \equiv k_{max}/N$ with the maximum degree $k_{max} \equiv \max_{1 \leq j \leq N} k_j$. The critical coupling strength is considerably decreased by the inactivation of low-degree nodes, i.e. $K_c^{het,l} < K_c^{het}$. On the other hand, the inactivation of the high-degree nodes (hubs) makes heterogeneous networks slightly more robust as compared with the random inactivation. This is because active oscillators with higher degree contribute less to the order parameter (see Fig. 2a). In this case, the critical coupling strength indicated in Fig. 5a is given by $K_c^{het,h} = a/d_{min} \sim K_c^{het}$. The difference between the critical ratio p_c

for random inactivation and that for targeted inactivation of high-degree nodes is subtle, as shown in Figs. 4a and 4d.

Discussion

We have demonstrated that heterogeneous networks are highly tolerant to random inactivation but extremely fragile to targeted inactivation of low-degree oscillators with respect to the dynamical robustness. The former property is consistent with the structural robustness of heterogeneous networks¹⁴. The latter property sheds light on the critical difference between the structural robustness and the dynamical robustness. These properties also hold for coupled oscillator models in which the coupling strengths are not identical but uniformly or normally distributed (see Supplementary Information). Our finding results from the diffusive coupling that serves to balance the states of the two connected nodes. Active nodes function to restore neighboring inactive nodes, with a resulting weakening of their dynamical activity. Because low-degree active nodes are affected by only a few neighboring inactive nodes, they can maintain relatively high dynamical activity compared with high-degree active nodes. Therefore, targeted inactivation of low-degree nodes leads to a considerable reduction in the network dynamical activity, making the network dynamically vulnerable.

This mechanism is expected to be applicable to a wide range of networked systems, because diffusion in various transport phenomena are commonly found in physical, biological, and engineering systems. For example, electrical synapses or gap junctions that are widely observed in the brain⁴¹ can be modeled by diffusive coupling in neural networks⁴²; in particular, rhythmicity and synchrony among inferior olive neurons⁴³ can be quantitatively described by a neural network model composed of oscillatory neurons coupled through such electrical synapses⁴⁴. Electric power networks that are composed of distributed power sources including renewable energy sources with inverters^{45,46} such as wind and solar power can also be modeled as a coupled oscillator network³³ interconnected by diffusive coupling with active and reactive power flows.

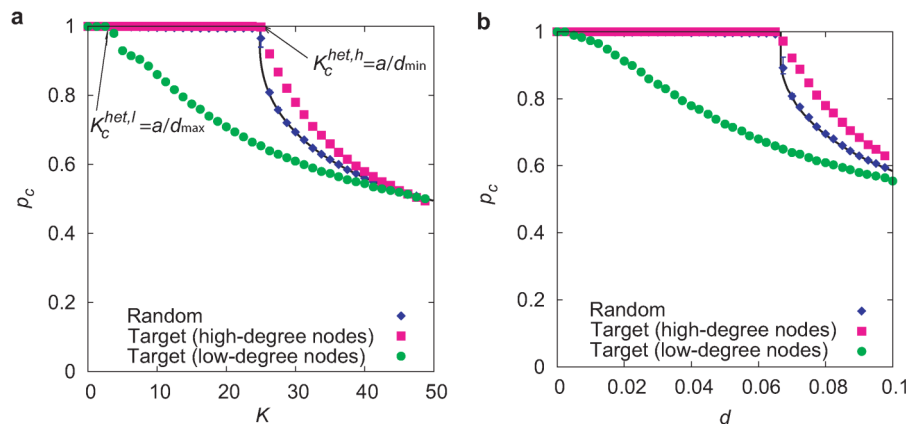


Figure 5 | Comparison of the critical ratio with respect to coupling strength K and link density d between random and targeted inactivation in heterogeneous networks. (a) The critical ratio p_c is plotted against the coupling strength K in heterogeneous networks with $d \sim 0.08$ ($N = 3000$ and $\langle k \rangle = 240$), $d_{max} \sim 0.3$, and $d_{min} \sim 0.04$. Blue diamonds and the black solid curve indicate the numerically and theoretically obtained critical ratios for random inactivation, respectively. Green circles and pink squares indicate the critical ratios for the targeted inactivation of low-degree and high-degree nodes, respectively. The critical coupling strength is given by $K_c^{het,l} \sim 3.3$ for the former case and $K_c^{het,h} \sim 25$ for the latter case, as theoretically predicted. (b) The critical ratio p_c is plotted against the link density d in heterogeneous networks with $N = 3000$ and $K = 30$.

Our results imply that dynamical processes play an important role in understanding the dynamical robustness in complex networks composed of interacting dynamical units. One needs to appropriately model dynamical processes and define a measure of dynamics-based network function to mathematically treat the dynamical robustness in such realworld networks as biological cellular networks^{11,21}, metabolic networks⁹, protein networks¹⁰, brain networks⁴⁷, and electric power networks⁴⁸. For designing dynamically robust networks and planning recovery strategies against local errors, both the network structure and the dynamical processes should be considered in detail.

Methods

Model equations. The network of diffusively coupled oscillators is described as follows:

$$\dot{z}_j = \left(\alpha_j + i\Omega - |z_j|^2 \right) z_j + \frac{K}{N} \sum_{k=1}^N A_{jk} (z_k - z_j) \quad \text{for } j = 1, \dots, N, \quad (3)$$

where N is the number of oscillators; z_j , the complex state variable of the j th oscillator; α_j , the intrinsic parameter of the j th oscillator; Ω , the natural frequency; and K , the coupling strength. The single oscillator without coupling ($K = 0$), called the Stuart-Landau oscillator²⁴, represents the normal form of dynamical systems that describe the nonlinear dynamics near the supercritical Hopf bifurcation at $\alpha_j = 0$ ⁴⁹. The single oscillator exhibits periodic (active) oscillation for a positive value of α_j , whereas it becomes quiescent (inactive) for a negative value of α_j (see Fig. 1a). The set of node indices for the active oscillators is denoted by S_A and that for the inactive oscillators, by S_I . We set $\alpha_j = a > 0$ for $j \in S_A$ and $\alpha_j = -b < 0$ for $j \in S_I$ ^{36,37}. The parameter values are fixed at $a = 1$, $b = 3$, and $\Omega = 3$. The adjacency matrix $A = (A_{jk})$ represents the network connectivity, where $A_{jk} = A_{kj} = 1$ if the j th and the k th oscillators are connected and $A_{jk} = A_{kj} = 0$ otherwise. The degree of the j th oscillator is given by $k_j = \sum_{k=1}^N A_{jk}$. The homogeneous and heterogeneous networks are given by the Erdős-Rényi random graph⁴ and the Barabási-Albert scale-free model⁶, respectively.

Order parameter and critical ratio. The macroscopic oscillation level of the entire network is evaluated by the order parameter $|Z|$, where $Z \equiv (1/N) \sum_{j=1}^N z_j$. When all the oscillators stop oscillating, the order parameter vanishes. As the ratio p of inactive oscillators increases from zero, the order parameter decreases and vanishes at a critical ratio $p = p_c$ (see Figs. 2b and 2d). In simulation experiments, the model equation (3) with random initial conditions was numerically integrated by the fourth-order Runge-Kutta method with time step 0.1, and the order parameter $|Z|$ was calculated at $t = 50000$. We considered the critical value p_c to be the value of p at which the value of $|Z|$ at $t = 50000$ falls below 10^{-6} as p is increased.

Mean field approximation. The critical ratio for random inactivation is analytically obtained by the mean field approximation^{38,39} or the annealed network approximation⁴⁰. The sum of contributions to the j th oscillator from the connected oscillators in Eq. (3) is represented by the local field $h_j \equiv \sum_{k=1}^N A_{jk} z_k$. For sufficiently large N , the number of active oscillators in the neighborhood of the j th oscillator is expected to be $(1-p)k_j$ and that of inactive ones, pk_j . Therefore, based on numerical

observations (see Supplementary Information), we approximate the local field as follows:

$$h_j(t) \simeq (1-p)k_j H_A(t) + pk_j H_I(t),$$

where the degree-weighted mean fields $H_A(t)$ and $H_I(t)$ for active and inactive subpopulations are given by

$$H_A(t) \equiv \frac{\sum_{j \in S_A} k_j z_j(t)}{\sum_{j \in S_A} k_j} \quad \text{and} \quad H_I(t) \equiv \frac{\sum_{j \in S_I} k_j z_j(t)}{\sum_{j \in S_I} k_j}. \quad (4)$$

Accordingly, the original equation (3) can be approximated as follows:

$$\dot{z}_j = \left(\alpha_j + i\Omega - |z_j|^2 \right) z_j + \frac{Kk_j}{N} \left((1-p)H_A(t) + pH_I(t) - z_j \right). \quad (5)$$

The coupling term, which is dependent on the connectivity matrix A_{jk} in the original equation, is now only dependent on the degree of the node. Once the mean fields H_A and H_I are provided, the steady oscillatory state of the j th oscillator is obtained from the reduced form (5). For the mean field approximation to be self-consistent, the mean fields calculated by equation (4) from the steady oscillatory states must be equivalent to the originally given mean fields. From a self-consistency analysis (see Supplementary Information), we derive the critical ratio (1) with

$$F(K, \alpha) \equiv \frac{1}{N} \sum_{j=1}^N \frac{d_j^2}{d_j - \alpha/K}, \quad (6)$$

where $d_j = k_j/N$ is the degree of the j th oscillator, normalized by the system size.

For homogeneous networks, we further assume that the degrees of all the oscillators are the same as the mean degree, i.e. $k_j = \langle k \rangle = (1/N) \sum_j k_j$ for all j . Then, because $d_j = d = \langle k \rangle/N$ for all j , equation (6) is reduced to $F(K, \alpha) = d^2/(d - \alpha/K)$. By substituting this form into equation (1), we obtain equation (2). See Supplementary Information for further details.

- Albert, R. & Barabási, A.-L. Statistical mechanics of complex networks. *Rev. Mod. Phys.* **74**, 1, 47–97 (2002).
- Newman, M. E. J. The structure and function of complex networks. *SIAM Review* **45**, 167–256 (2003).
- Boccaletti, S., Latora, V., Moreno, Y., Chavez, M. & Hwang, D.-U. Complex networks: structure and dynamics. *Phys. Rep.* **424**, 175–308 (2006).
- Erdős, P. & Rényi, A. On the evolution of random graphs. *Publications of the Mathematical Institute of the Hungarian Academy of Sciences* **5**, 17–61 (1960).
- Watts, D. J. & Strogatz, S. H. Collective dynamics of ‘small-world’ networks. *Nature* **393**, 440–442 (1998).
- Barabási, A. L. & Albert, R. Emergence of scaling in random networks. *Science* **286**, 5439, 509–512 (1999).
- Redner, S. How popular is your paper? An empirical study of the citation distribution. *Euro. Phys. J. B* **4**, 131–134 (1998).
- Liljeros, F., Edling, C. R., Amaral, L. A. N., Stanley, H. E. & Aberg, Y. The web of human sexual contacts. *Nature* **411**, 907–908 (2001).
- Jeong, H., Tombor, B., Albert, R., Oltvai, Z. N. & Barabási, A.-L. The large-scale organization of metabolic networks. *Nature* **407**, 651–654 (2000).
- Jeong, H., Mason, S., Barabási, A. L. & Oltvai, Z. N. Lethality and centrality in protein networks. *Nature* **411**, 41–42 (2001).
- Albert, R. Scale-free networks in cell biology. *J. Cell Sci.* **118**, 4947–4957 (2005).



12. Albert, R., Jeong, H. & Barabási, A.-L. Diameter of the world wide web. *Nature* **401**, 130–131 (1999).
13. Pastor-Satorras, R. & Vespignani, A. *Evolution and Structure of the Internet*. (Cambridge University Press, 2004).
14. Albert, R., Jeong, H. & Barabási, A.-L. Error and attack tolerance of complex networks. *Nature* **406**, 378–382 (2000).
15. Callaway, D. S., Newman, M. E. J., Strogatz, S. H. & Watts, D. J. Network robustness and fragility: percolation on random graphs. *Phys. Rev. Lett.* **85**, 25, 5468–5471 (2000).
16. Cohen, R., Erez, K., ben Avraham, D. & Havlin, S. Resilience of the Internet to random breakdowns. *Phys. Rev. Lett.* **85**, 21, 4626–4628 (2000).
17. Cohen, R., Erez, K., ben Avraham, D. & Havlin, S. Breakdown of the Internet under intentional attack. *Phys. Rev. Lett.* **86**, 16, 3682–3685 (2001).
18. Watts, D. J. A simple model of global cascades on random networks. *Proc. Natl. Acad. Sci. USA* **99**, 9, 5766–5771 (2002).
19. Motter, A. E. & Lai, Y.-C. Cascade-based attacks on complex networks. *Phys. Rev. E* **66**, 065102(R) (2002).
20. Wang, X. F. & Xu, J. Cascading failures in coupled map lattices. *Phys. Rev. E* **70**, 056113 (2004).
21. Barabási, A.-L. & Oltvai, Z. N. Network biology: understanding the cell's functional organization. *Nature Rev. Genet.* **5**, 101–113 (2004).
22. Kitano, H. Biological robustness. *Nature Rev. Genet.* **5**, 826–837 (2004).
23. Winfree, A. T. *The Geometry of Biological Time*. (Springer, New York, 1980).
24. Kuramoto, Y. *Chemical Oscillations, Waves, and Turbulence*. (Springer-Verlag, 1984).
25. Strogatz, S. Exploring complex networks. *Nature* **410**, 268–276 (2001).
26. Welsh, D. K., Takahashi, J. S. & Kay, S. A. Suprachiasmatic nucleus: cell autonomy and network properties. *Annu. Rev. Physiol.* **72**, 551–577 (2010).
27. Webb, A. B., Angelo, N., Huettner, J. E. & Herzog, E. D. Intrinsic, nondeterministic circadian rhythm generation in identified mammalian neurons. *Proc. Natl. Acad. Sci. USA* **106**, 38, 16493–16498 (2009).
28. Aujard, F., Herzog, E. D. & Block, G. D. Circadian rhythms in firing rate of individual suprachiasmatic nucleus neurons from adult and middle-aged mice. *Neuroscience* **106**, 2, 255–261 (2001).
29. Bernard, S., Gonze, D., Čajavec, B., Herzog, H. & Kramer, A. Synchronization-induced rhythmicity of circadian oscillators in the suprachiasmatic nucleus. *PLoS Comput. Biol.* **3**, 4, 667–679 (2007).
30. Smolen, P., Rinzel, J. & Sherman, A. Why pancreatic islets burst but single β cells do not. *Biophys. J.* **64**, 1668–1680 (1993).
31. Kruse, K. & Jülicher, F. Oscillations in cell biology. *Curr. Opin. Cell Biol.* **17**, 20–26 (2005).
32. Chen, L., Wang, R., Li, C. & Aihara, K. *Modeling Biomolecular Networks in Cells: Structures and Dynamics*. (Springer-Verlag, 2010).
33. Filatrella, G., Nielsen, A. H. & Pedersen, N. F. Analysis of a power grid using a Kuramoto-like model. *Eur. Phys. J. B* **61**, 485–491 (2008).
34. Gellings, C. W. & Yeager, K. E. Transforming the electric infrastructure. *Phys. Today* **57**, 12, 45–51 (2004).
35. Fairley, P. The unruly power grid. *IEEE Spectrum* **41**, 8, 22–27 (2004).
36. Daido, H. & Nakanishi, K. Aging transition and universal scaling in oscillator networks. *Phys. Rev. Lett.* **93**, 10, 104101 (2004).
37. Morino, K., Tanaka, G. & Aihara, K. Robustness of multilayer oscillator networks. *Phys. Rev. E* **83**, 056208 (2011).
38. Pastor-Satorras, R. & Vespignani, A. Epidemic spreading in scale-free networks. *Phys. Rev. Lett.* **86**, 14, 3200–3203 (2001).
39. Nakao, H. & Mikhailov, A. S. Turing patterns in network-organized activator-inhibitor systems. *Nature Phys.* **6**, 544–550 (2010).
40. Dorogovtsev, S. N., Goltsev, A. V. & Mendes, J. F. F. Critical phenomena in complex networks. *Rev. Mod. Phys.* **80**, 4, 1275–1335 (2008).
41. Galarreta, M. & Hestrin, S. Electrical synapses between GABA-releasing interneurons. *Nat. Rev. Neurosci.* **2**, 425–433 (2001).
42. Aihara, K. & Tokuda, I. Possible neural coding with interevent intervals of synchronous firing. *Phys. Rev. E* **66**, 026212 (2002).
43. Lang, E. J., Sugihara, I. & Llinás, R. GABAergic modulation of complex spike activity by the cerebellar nucleoolivary pathway in rat. *J. Neurophysiol.* **76**, 1, 255–275 (1996).
44. Katori, Y., Lang, E. J., Onizuka, M., Kawato, M. & Aihara, K. Quantitative modeling of spatiotemporal dynamics of inferior olive neurons with a simple conductance-based model. *Int. J. Bifurcat. Chaos* **20**, 3, 583–603 (2010).
45. Blaabjerg, F., Teodorescu, R., Liserre, M. & Timbus, A. V. Overview of control and grid synchronization for distributed power generation systems. *IEEE Trans. Ind. Electron.* **53**, 5, 1398–1409 (2006).
46. Hikiyama, T., Sawada, T. & Funaki, T. Enhanced entrainment of synchronous inverters for distributed power sources. *IEICE Trans. Fund. Electr.* **E90**, 11, 2516–2525 (2007).
47. Bullmore, E. & Sporns, O. Complex brain networks: graph theoretical analysis of structural and functional systems. *Nat. Rev. Neurosci.* **10**, 186–198 (2009).
48. Albert, R., Albert, I. & Nakarado, G. L. Structural vulnerability of the North American power grid. *Phys. Rev. E* **69**, 025103(R) (2004).
49. Guckenheimer, J. & Holmes, P. *Nonlinear Oscillations, Dynamical Systems, and Bifurcations of Vector Fields*. (Springer, 1983).

Acknowledgments

The authors thank J. Almendral, T. Hikiyama, T. Kobayashi, H. Kori, N. Masuda, Y. Susuki, and K. Tsumoto for their valuable comments. This research was supported by the Aihara Innovative Mathematical Modelling Project, the Japan Society for the Promotion of Science (JSPS) through the “Funding Program for World-Leading Innovative R&D on Science and Technology (FIRST Program),” initiated by the Council for Science and Technology Policy (CSTP).

Author contributions

All authors conceived and designed the research. G.T. carried out the numerical experiments. G.T. and K.M. worked out the theoretical analyses. All authors wrote the manuscript.

Additional information

Supplementary information accompanies this paper at <http://www.nature.com/scientificreports>

Competing financial interests: The authors declare no competing financial interests.

License: This work is licensed under a Creative Commons Attribution-NonCommercial-ShareAlike 3.0 Unported License. To view a copy of this license, visit <http://creativecommons.org/licenses/by-nc-sa/3.0/>

How to cite this article: Tanaka, G., Morino, K. & Aihara, K. Dynamical robustness in complex networks: the crucial role of low-degree nodes. *Sci. Rep.* **2**, 232; DOI:10.1038/srep00232 (2012).